EXTRACTION FROM CYCLOTRONS

J.I.M. Botman and H.L. Hagedoorn
Eindhoven University of Technology, Cyclotron Laboratory, Eindhoven, The Netherlands

Abstract
Several methods of extraction of ions in cyclotrons, such as stripping extraction and resonance extraction, are considered. An extraction efficiency of nearly 100% can be achieved by providing a very high energy gain per turn or alternatively, for H^- cyclotrons, by stripping. Only simple models are used to explain certain extraction features. Orbit centre coordinates are introduced. Examples of extraction devices for several cyclotrons are given.

1. INTRODUCTION

There are various types of cyclotrons for different applications. Extraction mechanisms and extraction devices are naturally adapted to the specific use of these cyclotrons. One may differentiate between stripping extraction for H^- cyclotrons and the extraction of positive ions employing an electric septum and a magnetic channel. In general, positive-ion cyclotrons for analytical purpose such as element analysis or material characterization, or for nuclear physics, do not require a large beam current but, instead, need a good beam quality and energy resolution. Here mostly resonance extraction methods are employed.

For the production of short-lived radionuclides high beam currents are neccessary, not only because of favourable cost per unit of product, but also because of the short lifetime. Compact cyclotrons that accelerate positive ions for isotope production generally have a limit in extracted beam current of about 100 μA. (Separated-sector cyclotrons can generate a much higher external current.) The internal beam of such a cyclotron yields a spot of a few mm^2 on a target. This means that with an energy of 30 MeV a beam power of 3 kW may hit the electrodes. Given the geometry of the extraction electrodes this approaches the maximum allowable output, certainly if one wants to have a high reliability of machine operation. The availability of negative ion sources with high output has given the opportunity to accelerate beams with high intensities e.g. 500 μA, and extract them via stripping. Here, in general, requirements on beam quality are less important than for cyclotrons for analytical applications.

We consider several methods of extraction, using only simple theory, and we give examples of extraction devices. The general discussion is restricted to isochronous cyclotrons, unless synchrocyclotrons are mentioned explicitely. We will start, however, with an older idea of extraction for early synchrocyclotrons.

It may be noted that because of the expanding orbits, extraction from cyclotrons in general has somewhat different aspects than for example fast and slow extraction techniques for synchrotrons, although resonances are often exploited in both cases. Slow extraction for synchrocyclotrons does have similar features to that for synchrotrons, however.

General theory and information on extraction from cyclotrons has been given by Heikkinen, Joho, Hagedoorn and others [1–3].

2. ON DEFLECTION AT n = 1 IN THE SYNCHROCYCLOTRON

In this section we briefly consider a paper from 1951 by Hamilton and Lipkin [4], with the title given above, in which a method was proposed for extraction from early synchrocyclotrons.

The synchrocyclotrons used until then, with a purely rotationally symmetric magnetic field falling off slowly radially, had a low dee voltage, with a subsequent small turn separation. By providing a coherent precessional motion of the orbits (i.e. the orbit centres move slowly about the magnet axis) via a field error or via mispositioning of the ion source, a larger orbit separation near the deflector was obtained and an extraction efficiency (i.e. the ratio of extracted to internal current) of typically 10% was achieved. The precessional motion leads to a large energy spread of the extracted beam, via high frequency phase mixing (see section 4.4).

For a cylindrically symmetric field, radial and axial particle motion are governed by the well known relations of Kerst and Serber, yielding stable motion for $0 < n < 1$, with n the field index

$$n = -\frac{r_0}{B(r_0)}\left(\frac{dB}{dr}\right)_{r_0}$$

where $B(r_o)$ is the axial field at radius r_o [5]. Hamilton and Lipkin made a plot of $B(r)r$ versus r for the synchrocyclotron. The top of the curve represents the highest energy attainable, and also gives the radius for which $n = 1$. They proposed to accelerate beyond the point $n = 1$, to utilize the inherent radial instability beyond this, so that orbits are automatically radially separated.

Now consider radial oscillations. It is easy to show that for radial oscillation of particles about an equilibrium orbit at radius r_o and with maximum and minimum radius r_b and r_a

$$\frac{1}{r_b - r_a}\int_{r_a}^{r_b} (Br)dr = B(r_0)r_0$$

i.e. the particles have equal areas at either side of r_o in the Br versus r plot (Fig. 1a). Particles for which equal areas do not exist, such as in Fig. 1b, are extracted at escape point r_e. This can also be seen in Fig. 2, in which the equivalent potential well for radial oscillations is drawn. The 'energy levels' correspond to amplitudes of radial oscillations.

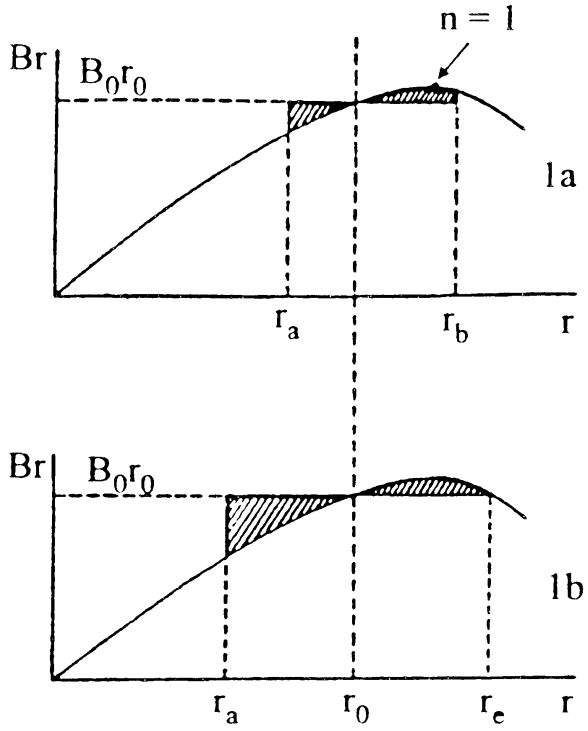

Fig. 1 (Br) versus r for the synchrocyclotron, with ranges of radial oscillations (see text)

Hamilton and Lipkin argued that the best situation is the one in which no coherent radial

oscillations exist throughout acceleration from source to final radius. This would lead to equal escape points for all particles, and equal final energy. As an example, for their cyclotron the value of *Br* at the $n = 1$ point is 8.5% above the value at $n = 0.2$ for which $\upsilon_r = 2\upsilon_z$, with υ_r and υ_z the radial and axial oscillation frequencies. (This coupling resonance could not be passed using the precessional extraction method because of energy exchange from radial to vertical motion and consequent beam loss.) Accordingly their final energy was higher. In present day thinking, for extraction one would provide a coherent oscillation amplitude near the $n = 0.2$ point, lifting the oscillation energy level from 1a to 1b in Fig. 2.

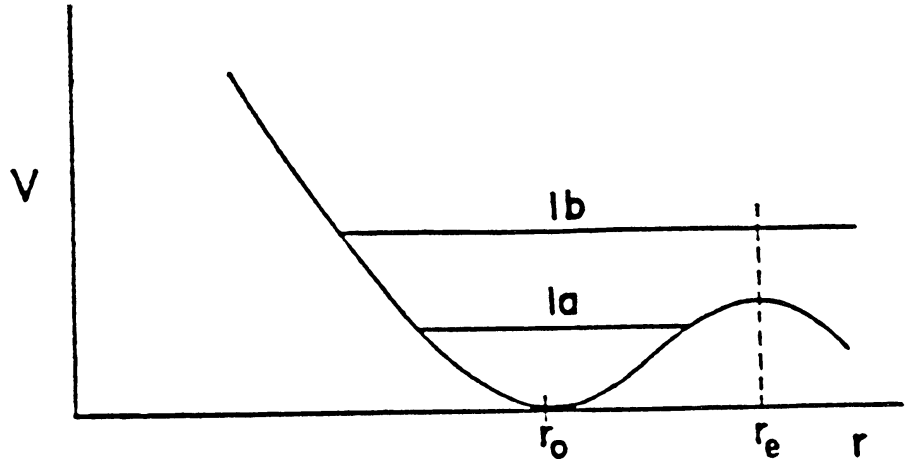

Fig. 2 Equivalent potential well for radial motion, and energy levels corresponding to situation in Figs. 1a and 1b.

3. STRIPPING EXTRACTION

During the last years the vast majority of commercially available cyclotrons serve to deliver proton beams in the energy range of 3 to 30 MeV [6]. They are mostly used for the production of short-lived radio-isotopes for medical diagnosis and for positron emission tomography. New areas of applications, such as neutron radiography, are being explored. Cyclotrons for pure nuclear physics are hardly built anymore, and if so their design is guided by the receiving laboratory. For these commercially available cyclotrons, it is advantageous to accelerate H^- beams, where convenient use can be made of stripping extraction, and where intensity problems, typical for the cyclotrons for analytical purposes or for nuclear physics, have been resolved. H^- cyclotrons are capable of accelerating particles with beam currents in excess of several 100 μA. Since 1975 the TRIUMF cyclotron, 520 MeV, 200 μA, is the well known big machine accelerating H^- beams, and employing extraction by stripping [7]. It is a major example in demonstrating the feasibility of H^- acceleration for isotope production cyclotrons.

In the extraction process the negative hydrogen ion beam simply passes a thin carbon foil (e.g. pyrolytic graphite, typically 50 to 200 $\mu g/cm^2$), which strips off the electrons. Figure 3 shows extraction orbits for the IBA Cyclone 30 cyclotron [8].

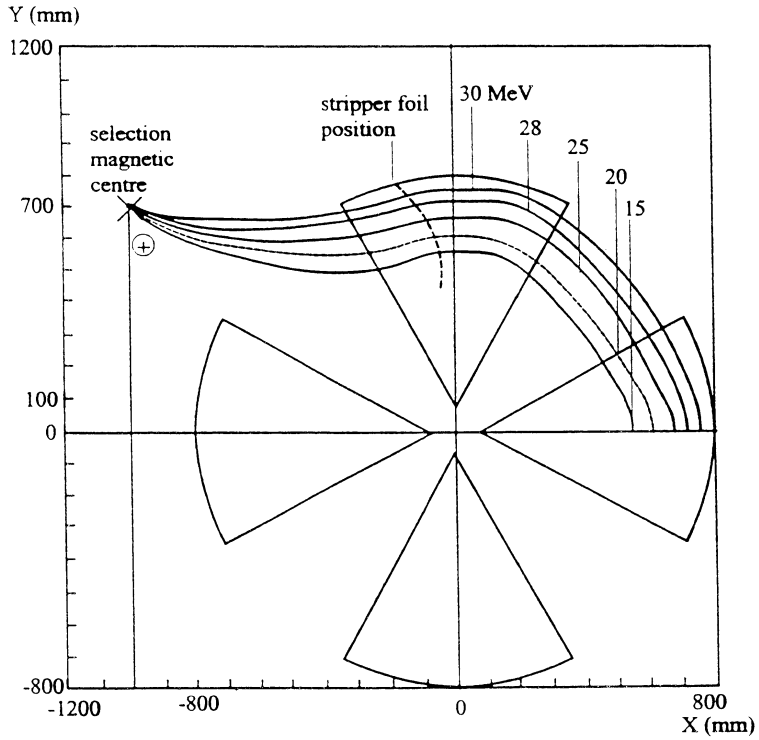

Fig, 3 Extraction orbits in the IBA Cyclone 30

3.1 Some important features of stripping extraction are:

- *a wide energy range may be covered by changing the foil position in the magnetic field (the precise foil position is defined by demanding a common cross over point outside the cyclotron magnet for extracted beams of different energies);*
- *at the cross over point, a combination magnet guides the beam into a single external beam transport line;*
- *a large internal beam currents can be handled, nowadays typically 300 to 500 μA, with 100% extraction efficiency; activation of cyclotron components is minimal, allowing machine access shortly after machine operation;*
- *the foil lifetime typically exceeds 2.10^4 μAh;*
- *the cyclotron fringe field is traversed with reversed rotation direction and with a large angle, hence there is no radial defocusing (which is a problem for extraction from positive-ion cyclotrons);*
- *simultaneous extraction of two beams to two external channels is possible with two foils corresponding to different energies and with different beam currents, e.g. for the production of two different isotopes at the same time.*

3.2 Energy spread

The energy spread of the extracted beam of H^- cyclotrons may be estimated as follows. Consider a radial phase space area at a radius r in the cyclotron, belonging to a kinetic energy T. This area just touches the stripper foil, see Fig. 4. We assume a good centreed beam in an ideal isochronous field. Particles lying in the part of the phase space area that overlaps with the foil are stripped and extracted from the cyclotron. Other particles have to make more revolutions to reach the stripper, and gain extra energy. As the energy is proportional to the radius squared [5], the energy spread of stripped particles is given by $\Delta T / T = 2\Delta r / r$ with Δr the radial width of the phase space area. As an example, for Δr = 5 mm at a radius of 500 mm the relative energy spread is 2%. Hence for achieving a small energy spread of the external beam it is of importance to have a good internal beam quality.

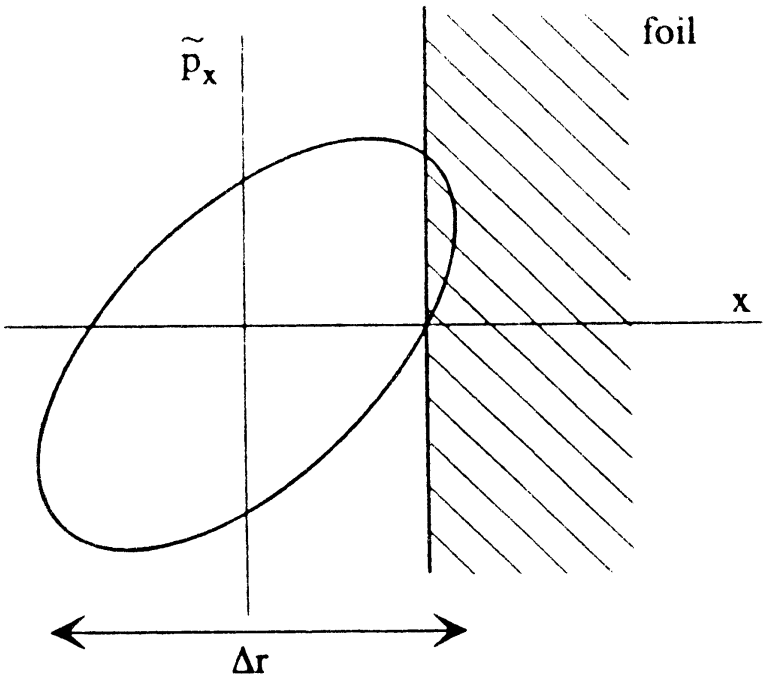

Fig. 4 Radial phase space area reaching the stripper foil

4. BEAM ORBITS

4.1 Orbit separation

Now we consider the extraction from cyclotrons with the help of extraction devices such as an electrostatic deflector, to direct the accelerated particles away from the cyclotron magnetic field. A large separation between successive turns is desired for reaching the highest extraction efficiency. In this section we give a simplified picture of orbit separation in a cyclotron, and we consider some methods to increase the separation [3,9].

Taking cylindrical coordinates, the radial position of a particle at an azimuth ϑ in the cyclotron, is given by:

$$r(\vartheta) = r_0(\vartheta) + x(\vartheta)\sin(\nu_r \vartheta + \vartheta_0) \ , \qquad (1)$$

where $r_O(\vartheta)$ is the radial position of the equilibrium orbit at that azimuth, $x(\vartheta)$ is the radial oscillation amplitude, and ϑ_0 is an arbitrary phase angle. For incoherent oscillations the amplitude $x(\vartheta)$ is given by

$$\sqrt{\beta_{r_0}(\vartheta)\epsilon_x} \ ,$$

with $\rho_{r_0}(\upsilon)$ the radial beta function for radius r_0 and at azimuth ϑ and ε_x the radial emittance. However, we now look at the radial position of the centre of the beam for a coherent oscillation, which has been induced by creating a field perturbation. Moreover we consider this at a fixed azimuth ϑ_i, i.e. the azimuth of the extractor entrance position. We restrict ourselves to the case of ν_r near 1; as $\nu_r \cong \gamma$ for isochronous cyclotrons, with γ the relativistic factor, this is the case for most cyclotrons. (The analysis can be adapted easily for the case of higher values of ν_r e.g. near 1.5 or 2.)

Rewriting Eq. (1), the radial position at $\vartheta_i = 2\pi n$ as a function of turnnumber n, is given by:

$$r(\vartheta_i) = r_0(\vartheta_i) \_ x\sin(2\pi n(\nu_r - 1) + \vartheta_0) \ , \qquad (2)$$

where for convenience ν_r-1 has been taken since ν_r is close to 1. The separation between two successive turns is:

$$\begin{aligned}\Delta r(\vartheta_i) &= \Delta r_0(\vartheta_i) + \Delta x \sin\left(2\pi n(\nu_r - 1) + \vartheta_0\right), \\ &+2\pi(\nu_r - 1)x\cos\left(2\pi n(\nu_r - 1) + \vartheta_0\right) .\end{aligned} \tag{3}$$

In this equation the three terms on the right-hand side represent the orbit separation due to different effects. We discuss them briefly, below.

The first term in Eq. (3) gives the orbit separation due to acceleration. The kinetic energy T of accelerated particles in the cyclotron is given by

$$T \propto \bar{r}^2 \bar{B}^2 ,$$

with $\bar{r}$ and $\bar{B}$ the average radius and field. Hence, neglecting the increase in the magnetic field, the turn separation due to acceleration is

$$\frac{\Delta \bar{r}}{\bar{r}} \cong \frac{1}{2}\frac{\Delta T}{T} ,$$

where ΔT is the energy gain per turn. As an example for a final energy of T = 30 MeV, ΔT = 100 keV, and an extraction radius of 0.5 m, we find $\Delta \bar{r} = 0.83$ mm. This is a rather small number, e.g. when compared with a radial beam width of for instance 4 mm.

Especially in separated sector cyclotrons with a high energy gain per turn, the turn separation near extraction due to acceleration may be sufficient. The PSI Injector II cyclotron [10] is a good example of this. At the extraction energy of 72 MeV the orbit separation is 1.9 cm, with an energy gain per turn of 1 MeV. In fact the large turn separation is also crucial as the machine is designed to handle currents in excess of 1 mA (the use of a flat-top cavity is also important here).

Apart from the turn separation by acceleration which is automatically present, there are two other mechanisms of forced separation which Eq. (3) reveals. The second term on the right-hand side in this equation gives the orbit separation by an increase in the oscillation amplitude. This can be accomplished by creating first or second harmonic magnetic field perturbations in a region where ν_r is close to 1:

$$B_p(x, \vartheta) = C_1(r)\cos\left(\vartheta - \psi_1(r)\right) + C_2(r)\cos\left(2\vartheta - \psi_2(r)\right)$$

where e.g. C_1 and ψ_{11} are the amplitude and phase of the first harmonic. This method can be regarded as providing dipole errors with closed-orbit distortions growing for tune values near integers, or providing gradient errors being most sensitive and leading to an increase in the beta function for half integer tune values [11]. This last method is the regenerative extraction method [12-14], and has been proposed and applied for synchrocyclotrons. Magnetic components called peeler and regenerator with positive and negative field gradients are introduced on certain azimuths in the cyclotron, and the tune enters the ν_r = 1 stopband. Moreover, in synchrocyclotrons one can program the RF such that the beam is stretched and that slow extraction can be applied [15]. So-called second harmonic extraction has been applied in a 14.5 MeV compact isochronous cyclotron [16], where the number of turns in the fringe field, where $\nu_r < 1$, was too small to allow making efficient use of the forced orbit separation enhancement mechanism discussed below.

4.4.1. Precessional extraction [3,17,18]

The coherent oscillation as given by Eq. (2) describes a precessional orbit motion with oscillation amplitude x. The turn separation due to precession is given by the third term on the right-hand side of Eq. (3); the maximum turn separation is given by $2\pi(\nu_r\text{-}1)x$. The effect is fully exploited by accelerating the beam far into the fringe field of the cyclotron, where $(\nu_r\text{-}1)$ has a substantial value. The side effect is that a higher final energy is reached in a given cyclotron field. As an example: when a coherent oscillation amplitude x of 3 mm has been built up (e.g. by a first harmonic perturbation near $\nu_r = 1$) and acceleration takes place until $\nu_r = 0.8$, the maximum turn separation due to precession is 3.8 mm. This can be added to the value of 0.83 mm of the example of separation by energy gain.

Accelerating the beam far into the fringe field often means passing the $\nu_r = 2\,\nu_z$ coupling resonance. Energy can be exchanged from the radial to the vertical motion, blowing up the beam vertically and leading to beam loss. If the radial oscillation amplitude is not too large, and if the resonance is passed in only a few revolutions, vertical amplitude increase is avoided [3]. In practice, a coherent radial oscillation amplitude of the same size as the incoherent amplitude, is a good criterion for efficient extraction. Another reason for requiring not too large radial oscillation is avoiding strong non linear effects.

4.2 The orbit centre

Radial oscillations of particles w.r.t. the equilibrium orbit can conveniently be described by the movement of their orbit centres, see Fig. 5. (In a Hamiltonian formulation of betatron oscillations in cyclotrons the orbit centre coordinates are the canonical coordinate and momentum.)

Denoting the angle deviation by $p_x = p_x / p_0$, where p_x is the transverse and p_0 is the overall momentum, the phase space area is equivalent to the area of orbit centres (x,y). The radial motion of a particle is represented by a slowly moving orbit centre motion. If $\nu_r = 1$ the orbit centre remains fixed in place; if $\nu_r - 1 > 0$ the orbit centre moves with frequency $-(\nu_r - 1)$, i.e. rotates opposite to the particle motion. The actual position of the particle is found by adding the radius of curvature of the equilibrium orbit at its azimuth to the orbit centre position.

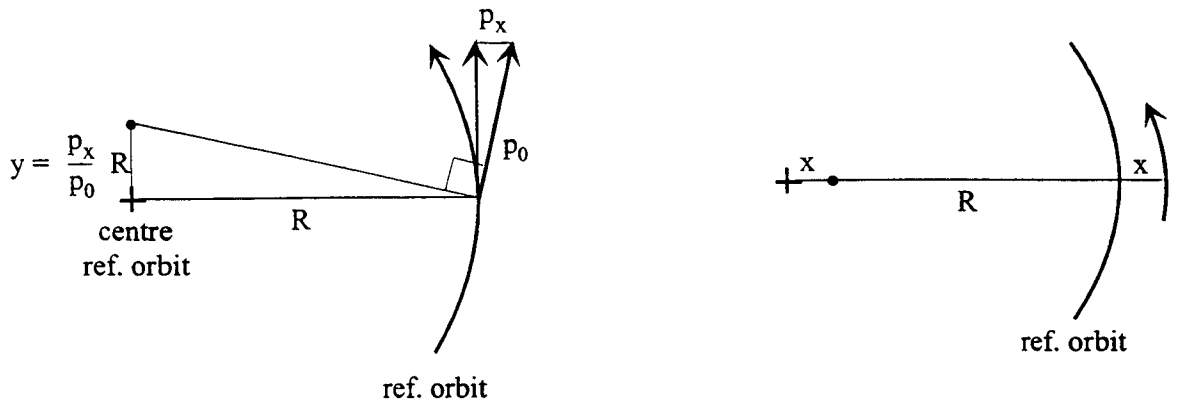

Fig. 5 Relation between orbit centre coordinates and position and radial momentum deviation of the particle from the central orbit

4.3 The effect of a 1st harmonic

We give an expression for the radial oscillation amplitude induced by a first harmonic field perturbation. Let a positive magnetic field bump ΔB extend over an azimuthal interval $\Delta\vartheta$ along the negative x-axis, let the particle motion be anticlockwise, and let $\nu_r > 1$ (see Fig 6).

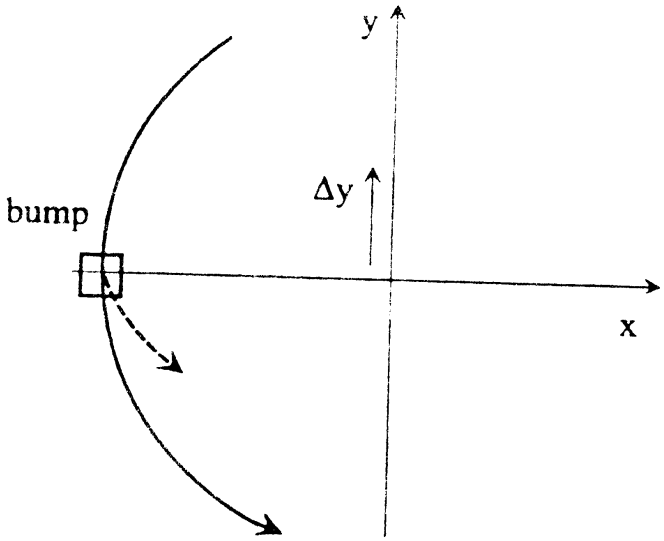

Fig. 6. Orbit centre shift Δy due to a magnetic field bump along the negative x-axis

The 1st harmonic is

$$A_1 = \frac{1}{\pi}\int_0^{\pi} \Delta B d\vartheta = \frac{\Delta\vartheta}{\pi}\Delta B \ .$$

The field bump gives a change in radial momentum:

$$\Delta\tilde{p}_x = \frac{\Delta B}{B}\Delta\vartheta$$

and an orbit centre shift:

$$\Delta y_1 = \frac{\Delta B}{B} R\Delta\vartheta \ .$$

In one turn a hypothetical particle with oscillation amplitude A, see Fig. 7, has its orbit centre displaced by:

$$\Delta y_2 = -2\pi\left(\nu_r - 1\right)A \ .$$

When $\Delta y_1 = \Delta y_2$ one finds a new equilibrium orbit, because the orbit is closed. The orbit centre of this equilibrium orbit (middle of the closed curve) is given by $\Delta x = A$. The beam starts oscillating around the new orbit centre. One finds:

$$\begin{aligned}\Delta x &= \frac{1}{2\pi\left(\nu_r - 1\right)}\frac{\Delta B}{B} R\Delta\vartheta \\ &= \frac{\epsilon_1 R}{2}\left(\nu_r - 1\right)^{-1}\end{aligned} \ ,$$

in which ε_1 is the relative first harmonic $\varepsilon_1 = A_1/B$.

Often

$$\Delta x = \frac{\epsilon_1 R}{\nu_r^2 - 1}$$

is given. Since (υ_r - 1) is small, this is about the same.

As an example: taking $\varepsilon_1 = 10^{-4}$, R = 1 m and υ_r - 1 = 0.01, one finds an orbit centre shift, i.e. a radial oscillation amplitude, of Δx = 5 mm.

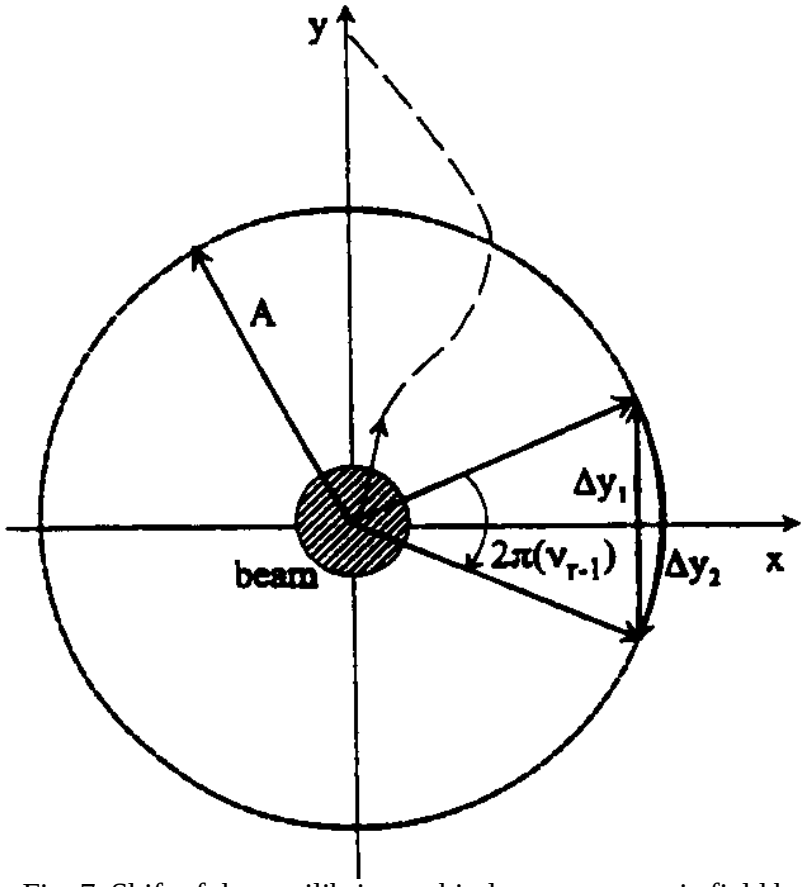

Fig. 7 Shift of the equilibrium orbit due to a magnetic field bump

4.4 HF phase mixing

When a coherent oscillation amplitude is given to the beam in the centre of the cyclotron, e.g. by an ion source position error, orbit centres at the final radius for particles with different HF phases ($ø_{HF}$) lie on a circular band. After n turns the orbit centre of a particle shifts by an angle:

$$\vartheta = 2\pi \int_0^{\pi} \left(\nu_r - 1\right)\, dn \ .$$

Particles with different HF phases have to make a different number of turns to reach the final radius. Hence the corresponding orbit centres have a different azimuth. This is the phenomenon of HF phase mixing. It implies a deteriorated beam quality and an increased energy spread of the extracted beam (see section 3).

In most cases in the precessional extraction process, where a coherent oscillation is induced on the passing of the ν_r = 1 resonance, the spreading of orbit centres for different HF phases due to HF mixing, is small for an originally well centreed beam, as in general the number of turns from the ν_r = 1 resonance till extraction is not so large. So in general the coherence of the radial oscillations persists for particles with a different HF phase. This is one of the favourable features of the precessional extraction method. In contrast to this, an example showing the orbit centre off-set for different HF phases has been given by Laxdall [19], (Fig. 8) in a study of H^- extraction from the TRIUMF cyclotron (with many turns from the

ν_r = 3/2 resonance till extraction).

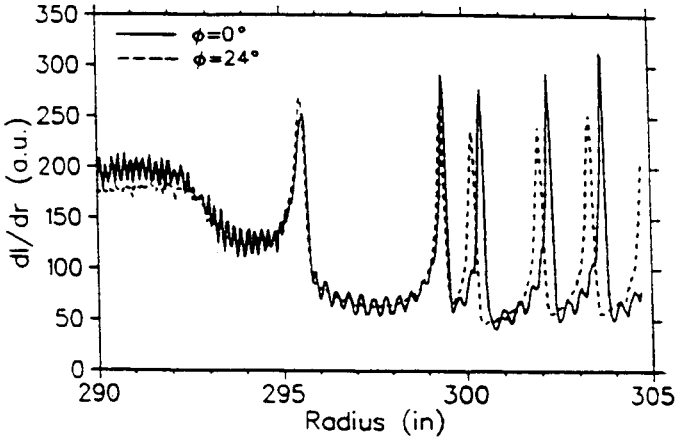

Fig. 8 Radial scans for the TRIUMF cyclotron using a differential probe showing the beam density pattern for an optimized phase band and for a phase band off-set by 24°. Phase dependent amplitude growth at the υ_r=3/2 resonance and a cosø dependence in the rate of advance of the precession centre account for the difference.

5. PRECESSIONAL EXTRACTION, NUMERICAL SIMULATION

In this section a numerical example regarding the precessional extraction method is presented, and some remarks about it are given [9]. The calculations refer to the AVF cyclotron of the Eindhoven University [20].

The equations of motion are integrated up to the extraction radius, starting before the ν_r = 1 radius. The measured magnetic field data are used, and a first harmonic field perturbation

$$\Delta B(r,\vartheta) = C_1(r)\cos\big(\vartheta - \psi_1(r)\big)$$

is included to provide a coherent oscillation at ν_r = 1. The tune diagram for the machine is given in Fig. 9, in which the average radius is indicated. The beam is extracted at and the calculations start at $\bar{r}$ = 48 cm.

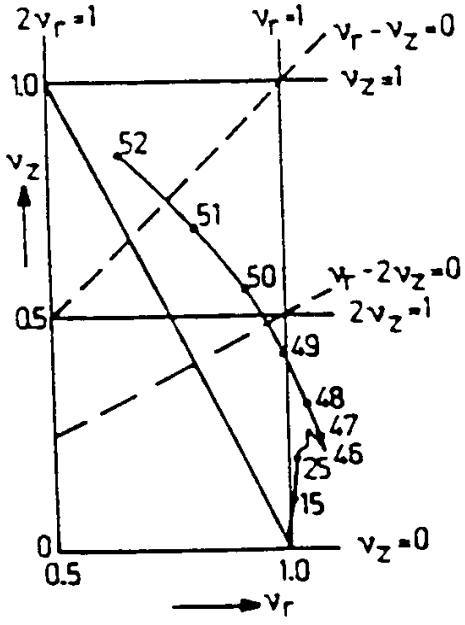

Fig.9 Tune diagram for the Eindhoven cyclotron, with the average radius indicated

It is seen that several resonances are passed during the extraction process, of which $\nu_r = 1$ and $\nu_r = 2\nu_z$ are the most important ones. Figure 10 gives the motion of a grid of particles in radial phase space.

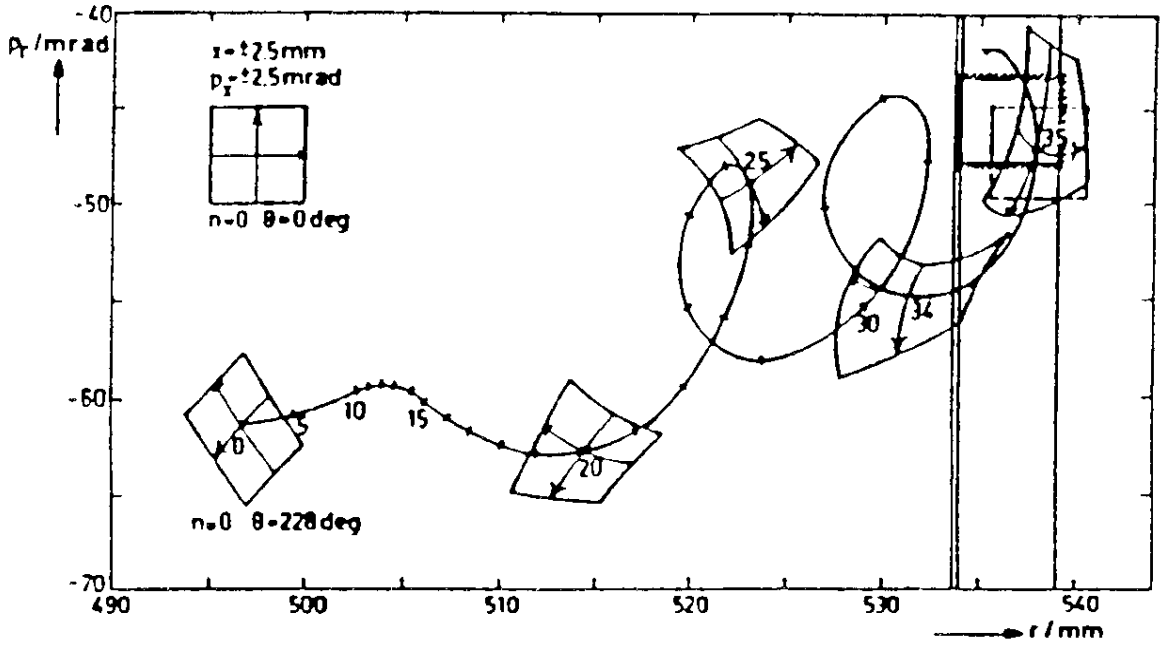

Fig. 10 Precessional extraction. Evolution of particles with $\phi_{HF} = 30^{\circ}$ in radial phase space for the Eindhoven cyclotron. The extractor aperture in phase space has been calculated (solid aperture); an optimum location is indicated (aperture in broken lines).

The following remarks and observations can be made:

- The calculation starts about 10 turns before $\nu_r = 1$, 'turn 0'.
- The entrance of the extractor (as indicated by a box) lies near a hill-valley boundary. Therefore the orbits are directed inwards by about 50 mrad. This explains the negative vertical scale.
- The turn separation is about 0.5 mm near $\nu_r = 1$. It increases rapidly.
- A cycloidal motion can be seen due to both acceleration and the presence of a radial oscillation.
- A coherent oscillation has been created with an amplitude of ~ 3 mm.
- Between $n = 26$ and $n = 32$ there is one radial oscillation. Hence $|\nu_r - 1| \cong 1/6$ or $\nu_r \approx 0.83$.
- There is a large beam separation between turn 34 and 35 of about 6.5 mm.
- The septum width (0.4 mm) and the deflector aperture are indicated. The turn separation is sufficient compared to the septum width.
- There is a non-linear distortion of the phase plane area.
- The energy spread of the extracted beam is about 2 eV_{dee}, which is the energy difference between turn 34 and 35, with V_{dee} the dee voltage (the cyclotron has a single-dee RF system).
- There is an energy position correlation along the cycloid, as this curve describes an oscillation about equilibrium orbits with increasing energy (or radius).
- Particles with another HF-phase ϕ_{HF} lie on the same cycloid, with more or less turns, to reach the extractor, as the HF-phase mixing is not effective, see section 4.4. With the remark above this implies the quoted energy spread of 2 eV_{dee} for the entire beam.

Figure 11 shows a differential probe measurement for this cyclotron in the extraction region. The separation between the probe fingers is 2 mm. The figure reveals the radial

oscillation near extraction.

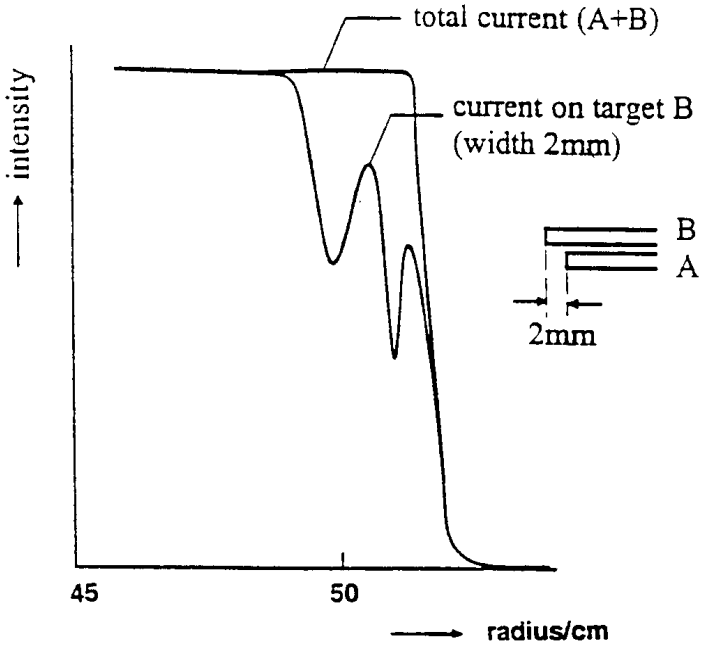

Fig. 11 Differential probe scan near extraction for the Eindhoven cyclotron

6. MULTI- AND SINGLE-TURN EXTRACTION

In general, particles with a different value of the HF-phase complete a different number of revolutions before reaching the extraction septum and having the final energy. In a purely isochronous machine the HF phase of a particle remains constant, which explains this. This leads to multi-turn extraction. For the Eindhoven cyclotron, as an example, the number of turns may vary by about 30, with a total number of about 300. Single-turn extraction on the other hand can be obtained when the HF phase width is restricted, e.g. with the help of slits in the centre of the cyclotron. This leads to a reduced energy spread of the extracted beam. Multi- and single-turn extraction has been described by several authors [21, 22].

The kinetic energy T and the radius r of particles on equilibrium orbits after N turns is given by:

$$T = T_0\left(1 - 1/2\phi^2\right) ,$$

$$r = r_0\left(1 - 1/4\phi^2\right) ,$$

where T_0 and r_0 belong to a central HF phase $ø_0$, and where ø is the phase difference with respect to $ø_0$. A plot of the energy for orbits near the extractor as a function of HF phase is given in Fig. 12. This figure also shows the energy levels belonging to the extractor opening, i.e. of the septum and the electrode. The top of the paraboles is shifted due to the effect of the fringe field. It is seen that several turns get extracted, with an energy pattern for the external beam as given in Fig. 13. Single-turn extraction is obtained for a phase width restricted to $Δø = ø_2 - ø_1$ (see Fig. 13), or for $|ø| < \arccos(N/N + 1)$.

For example with $N = 180$, $|ø| < 6^\circ$, single-turn extraction for a wider phase range and with a small resulting energy spread can be obtained by applying a higher harmonic cavity in addition to the fundamental RF frequency. This is the flat-topping principle [5]. Important examples of this are found in the PSI injector II and ring cyclotrons [10,23]. The additional advantage is of course the possibility to extract the beam with 100% efficiency. In Eindhoven a special minicyclotron (ILEC) has been constructed with an RF phase acceptance five times larger due to the flat-topping technique, and an energy spread less than 0.1% [24]. This

machine serves especially for PIXE and PIXE microbeam applications.

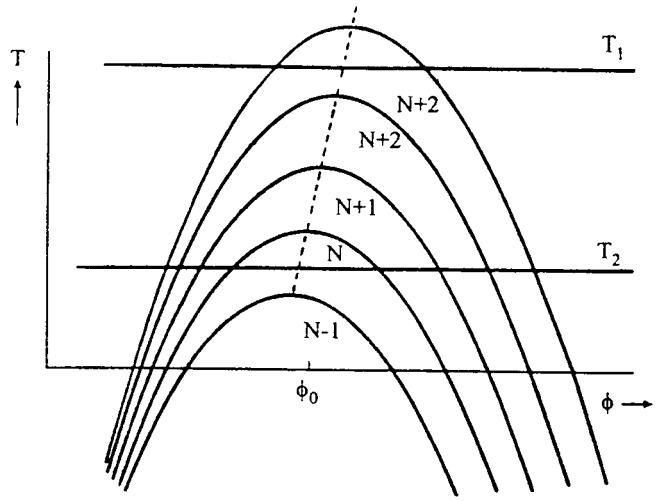

Fig. 12 Kinetic energy versus HF phase near extraction

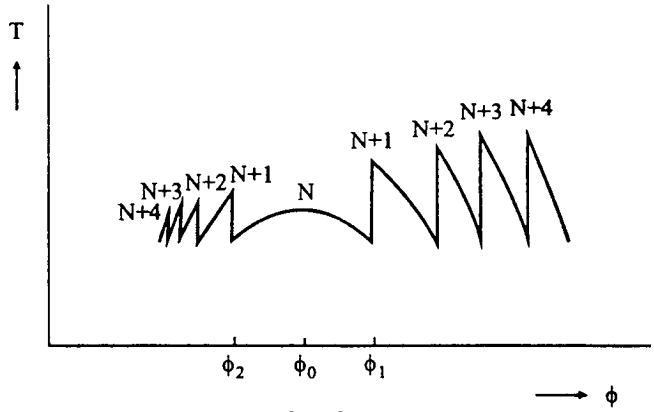

Fig. 13 Energy profile for the extracted beam

For the main Eindhoven cyclotron, which is a multiturn machine, single-turn experiments have been made by restricting the RF phase width with radially selecting slits in the cyclotron centre [25]. The accelerating voltage was set to have about 180 turns, hence the phase width had to be within 12˚. Single-turn extraction was found by observing 100% variation in the external beam current as a function of the accelerating voltage, see Fig. 14. This implies that the

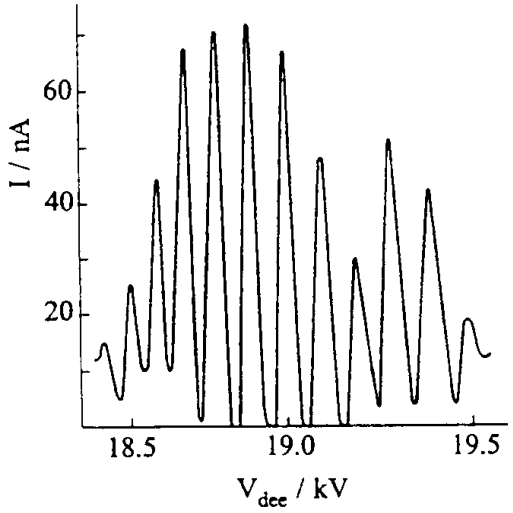

Fig. 14 Single-turn extraction demonstrated by 100% external beam variations as a function of accelerating voltage

number of turns in the cyclotron can be selected. In this situation the FWHM relative energy spread of the external beam is 0.85 10^{-3}, compared to 0.310^{-2} for multiturn extraction. The single-turn effect is extremely sensitive to variations in the magnetic field, e.g. a variation of $\Delta B/B = 2.10^{-4}$ of the main magnetic field destroys the single-turn extraction. However, in this situation the effect of a first-harmonic field perturbation in the centre of the cyclotron created by the inner harmonic coils, could be compensated rather completely by a first harmonic of the outer harmonic coils. Increasing the beam current through the slits destroys the single-turn extraction: space charge effects at low energy increase the RF phase width.

7. DEFLECTION DEVICES

The extraction hardware for a cyclotron usually consists of an electrostatic deflector followed by a magnetic channel. The curvature of the electrodes of the deflector must correspond to the shape of the orbits of extracted ions. An angle kick of typically 50 to 100 mrad is provided. The inner electrode, septum, is at earth potential. At the entrance it has a thickness of a few tenths of a mm, increasing to several mm at the exit. A V-slit at the entrance is often used to distribute the deposited power over a larger area. The septum is water cooled.

Smith and Grunder [26] have given a criterion for the product of electric field E and potential V for a cyclotron deflector in order to avoid electric discharges: $VE < 1.5\ 10^4$ $(kV)^2/cm$. This is shown in Fig. 15 together with deflector voltage values for several cyclotrons. The maximum sustainable voltage in a magnetic field is 20-30% lower than without magnetic field [27].

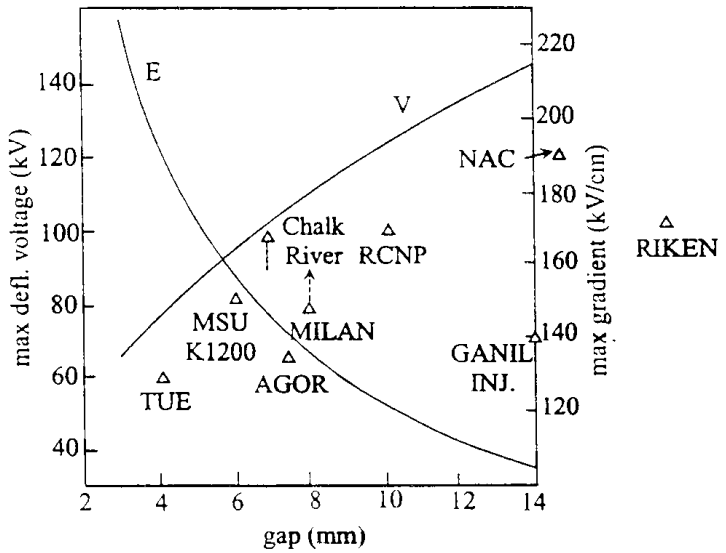

Fig. 15 Maximum electric field and voltage as a function of the deflector gap for cyclotron deflectors. The operating deflector voltage for several cyclotrons has been indicated.

In order to reduce the cyclotron magnetic field along the extraction paths and to provide a horizontally focusing action for compensating the defocusing action of the cyclotron fringe field, passive [28] or active [29] magnetic channels are employed. In the design of a magnetic channel it is important that it's magnetic field is strongly decreased in the area of the last accelerated orbits.

Figure 16 shows a passive magnetic channel which is housed within the accelerating electrode of the ILEC cyclotron [24]. Figure 17 shows the extraction elements in the AGOR cyclotron [30], consisting of an electrostatic deflector ESD, an active normal conducting channel EMC1, and a superconducting channel EMC2. Moreover two superconducting focusing and steering elements are located on the passage of the magnet yoke. Figure 18 gives the conductor arrangement for the EMC1.

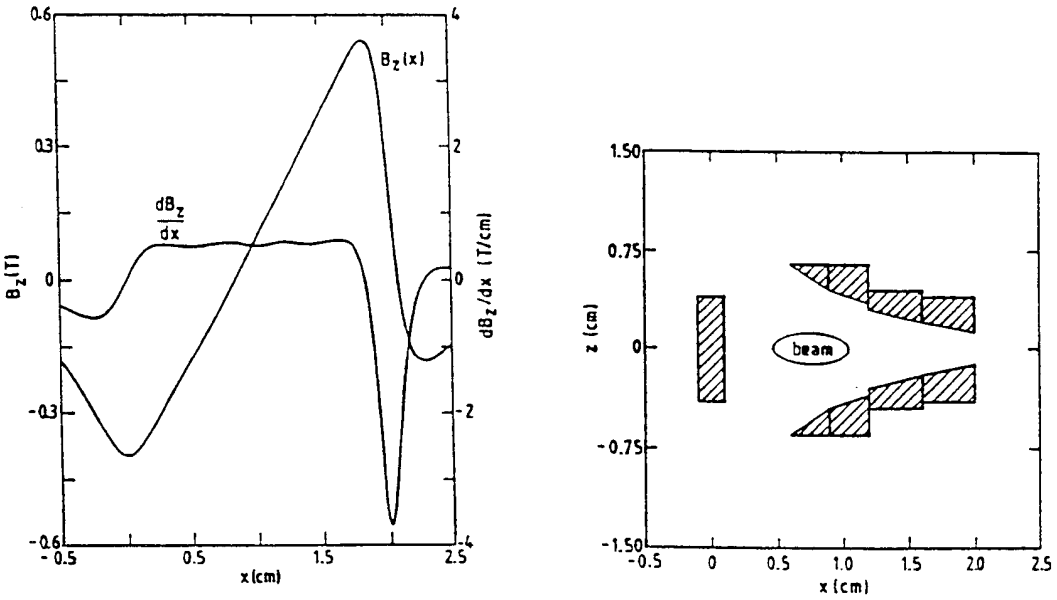

Fig. 16 Calculated magnetic field and its gradient as produced by a passive magnetic focussing channel in the ILEC cyclotron. The figure also shows a vertical cross-section through the channel.

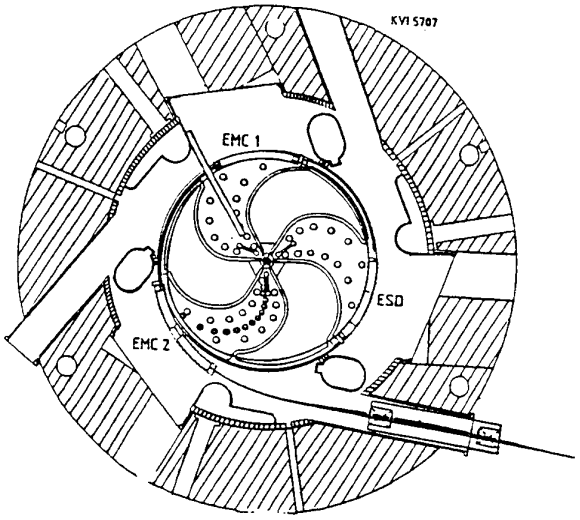

Fig. 17 Median plane view of the AGOR cyclotron with its extraction elements

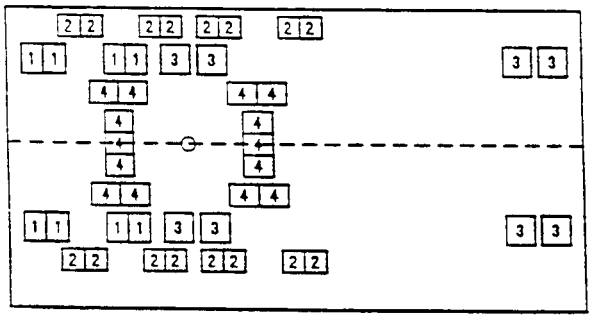

Fig. 18 Cross-section of the conductors of EMCl. The cyclotron centre is at the left, the circle marks the axis of the extracted beam. The distance between conductors 4 is about 1.5 cm
4: deflecting coil $\Delta B \leq 0.2$ T; 2: gradient coil $dB/dx \leq 13$ T/m; 3: compensation of stray field at long range; 1: compensation of stray field at short range

8 . CONCLUSION

Several methods of extraction from (isochronous) cyclotrons have been discussed. Most important are stripping extraction, resonance free and precessional extraction. Some hardware aspects have been given.

ACKNOWLEDGEMENTS

We thank W. Kleeven (IBA), M. Kruip (Oxford Instruments), H. Schreuder (KVI) and Bob Laxdall (TRIUMF) for useful information and comments.

REFERENCES

[1] P. Heikkingen, Injection and extraction for cyclotrons, CAS, CERN 94-01,Vol. II, (1994), 819.

[2] W. Joho, Extraction from medium and high energy cyclotrons, Proc. 5 Int. Conf. on Cycl., Butterworths, London, (1971), 159.

[3] H.L. Hagedoorn and P. Kramer, Extraction studies in an AVF cyclotron, IEEE Trans. Nucl. Sci. NS-13, No. 4, (1966), 64.

[4] D.R. Hamilton and H.J. Lipkin, On deflection at n = 1 in the synchrocyclotron, Rev. Sci. Instr., Vol. 22, No. 10 (1951), 783.

[5] T. Stammbach, Introduction to cyclotrons, these proceedings.

[6] V. Bechtold, Commercially available compact cyclotrons for isotope production, Proc. 13 Int. Conf. on Cycl., Vancouver 1992, World Scientific, (1993), 110.

[7] G. Dutto, The TRIUMF 520 MeV cyclotron, Ibid, 138.

[8] Y. Jongen et. al., Construction of the Louvain La Neuve 30 MeV 500 μA H^-cyclotron, Proc. 11 Int. Conf. on Cycl., Ionics, Tokyo, (1987), 275.

[9] F. Schutte et. al., Numerical calculations in the extraction process of the Eindhoven AVF cyclotron, Nucl. Instr. Meth. 127, (1975), 317.

[10] U. Schryber et. al., Status report on the new injector at SIN, 9 Int. Conf. on Cycl., Les Edition de Physique (France), (1981), 43.

[11] E. Wilson, Transverse beam dynamics, CAS, CERN 94-01, Vol. I., (1994), 131.

[12] J.L. Tuck and L.C. Teng, Regenerative deflector for synchrocyclotrons, Phys. Rev. 81, (1951), 305.

[13] K.J. Le Couteur, The regenerative deflector for synchrocyclotrons, Proc. Phys. Soc. London, B64, (1981), 1073.

[14] N.F. Verster, Regenerative extraction from the 150 MeV synchrocyclotron at the Laboratoire Curie, IICC, (1959), 224.

[15] D.W. Storm, A survey of synchrocyclotron projects, IEEE Trans. Nucl. Sci., Vol. NS-26, No. 2, (1979), 1970.

[16] J.M. van Nieuwland, Extraction of particles from a compact isochronous cyclotron, Thesis TU Eindhoven, (1972).

[17] H.L. Hagedoorn and N.F. Verster, The extraction of the beam of the Philips AVF cyclotron, CERN 63-19, (1963), 228.

[18] M.M. Gordon and H.H. Blosser, Orbit calculations on the extraction system for the MSU cyclotron, Ibid, 236.

[19] R.E. Laxdall et.al., Beam test results using the auxilary accelerating cavity, Proc. 13 Int. Conf. on Cycl., World Scientific, (1992), 442.

[20] N.F. Verster et. al., The Philips prototype AVF cyclotron, CERN 63-19, (1963), 43.

[21] M.M. Gordon, Single turn extraction, IEEE Trans. Nucl. Sci. NS-13, No. 4, (1966), 48.

[22] H.L. Hagedoorn et. al., Some factors determining the beam quality of AVF cyclotrons, Proc. 5 Int. Conf. on Cycl., Butterworths, London, (1971), 274.

[23] Th. Stammbach, Experience with the high current operation of the PSI cyclotron facility, Proc. 13 Int. Conf. on Cycl., World Scientific, (1992), 28.

[24] W.J.G.M. Kleeven, Theory of accelerated orbits and space charge effects in an AVF cyclotron, Thesis Eindhoven University, (1988).

[25] J.I.M. Botman, Central region study for a moderate energy cyclotron, Thesis Eindhoven `University, (1981).

[26] B.H. Smith and H.A. Grunder, Electrical design of electrostatic deflectors for sector-focused cyclotrons, CERN 63-19, (1963), 304.

[27] F. Broggi et. al., The electrostatic deflectors for the Milan superconducting cyclotron, 12 Int. Conf. on Cycl., Word Scientific, (1991), 350.

[28] G. Bellomo, Design of passive magnetic channels, 13 Int. Conf. on Cycl., World Scientific, (1992), 592.

[29] K. Pieterman et. al., The AGOR superconducting extraction channel EMC2, ibid., 585.

[30] H.W. Schreuder, The AGOR cyclotron past the half-way mark, 13 Int. Conf. on Cycl., World Scientific, (1992), 21.